Soft Matter

Accepted Manuscript

ROYAL SOCIETY OF CHEMISTRY

www.rsc.org/softmatter

Journal Name

RSCPublishing

ARTICLE

Functionality-Oriented Molecular Gels: Synthesis and Properties of Nitrobenzoxadiazole (NBD)-containing Low-molecular Mass Gelators

Cite this: DOI: 10.1039/x0xx00000x

Received 00th January 2012,
Accepted 00th January 2012

DOI: 10.1039/x0xx00000x

www.rsc.org/

Hang Yu, Yanchao Lü, Xiangli Chen, Kaiqiang Liu, Yu Fang*

Two nitrobenzoxadiazole (NBD)-containing cholesteryl (Chol) derivatives were prepared by introducing D/L-phenylalanine into the linkers between the NBD and Chol units. The compounds were denoted as **NLC** and **NDC**, respectively. The gelation behaviors of them were tested in 34 liquids. It was found that the chirality of the linkers shows great effect on the gelation ability and the gel properties of the two compounds. SEM studies demonstrated that the gelator in the gel of **NDC**/DMSO aggregated into uniform fibrous structures. FTIR, ^{1}H NMR and UV-Vis spectroscopy measurements revealed that intermolecular hydrogen bonding and π-π stacking are two main driving forces to promote the gel formation. Interestingly, the **NDC**/DMSO gel exhibits rapid and reproducible gel-sol phase transition and fluorescence quenching upon introduction of ammonia. Furthermore, both the gel and the fluorescence emission could be fully recovered upon evaporation of the ammonia gas introduced. Spectroscopy and model system studies revealed the association of ammonia with the nitro group of the NBD unit of the compound, which is recognized as the main reason for the chemical responses of the gel system. On the basis of the discovery, an ammonia sensing film had been fabricated and made into device. Furthermore, the device-based and conceptual "ammonia leaking" monitoring instrument was developed. Preliminary test demonstrated that the performance of the system is exceptional good, a typical and persuasive example to show the important real-life applications of molecular gels.

Introduction

Gels are everywhere due to it's a wide range of applications in cosmetics, sensor technology, conservation of arts, drug delivery and biomedical applications etc.[1-5] For realizing and/or enhancing gelation, saccharide, ureido and steroidal structures etc. have been employed as important building blocks in the creation of low-molecular mass compounds-based gelators (LMMGs). [6-8] However, these structural elements are usually optical inactive, which may limit some specific applications of the relevant gels. [9] Furthermore, considering the fact that molecular gel formation is a self-assembling process of LMMGs, and in other words the molecules of gelators in gel-networks are relatively in low entropy state or high degree of ordered state, it may be reasonable to anticipate that combination of weak interaction-based organization and fluorescence property of LMMGs in molecular gels may bring opportunities for creating novel stimuli-responsive, including sensing, systems. [10-13]

Stimuli-responsive gels have been seen as a new kind of responsive materials, because they combine the elastic behavior of solids with the micro-viscous properties of fluids. Compared with chemical gels, of which the gel networks are maintained by cross-linked covalent bonds, physical gels are built by non-covalent interactions such as hydrogen bonding, π-π stacking, van der Waals interaction, host-guest interaction and electrostatic interaction, etc.[14-16] It is the difference in the bonding nature of the gel networks that makes physical gels rather than chemical gels have been chosen as responsive systems in smart materials research.

The stimuli for responsive gels can be devided into physical stimuli and chemical stimuli. Temperature, mechanical stress, light illumination, sonication, magnetic field are the main physical triggers that gels can response to.[17-19] On the contrary, chemical stimuli are mainly pH variation due to addition of acids or bases, oxidation/reduction due to introduction of oxidants or reductants, and chemical reaction via addition of other chemicals.[19-21] In the past few decades, several LMMGs-based gel systems have been reported for their responses to chemical stimuli. Huang and co-workers reported some self-healing molecular gels based on a host-guest interaction.[22] Due to the pH-controllable properties of the host-guest recognition motif, the gels they obtained can act as degradable materials triggered by pH stimuli. Chen and co-workers obtained a cationic sensitive gel, and developed metal ion sensors by using the gel.[23] Weiss and colleagues prepared a class of molecular gels, and demonstrated that the gels are responsive to CO_2.[24] The gels, however, could be rebuilt by displacing the gas with N_2.

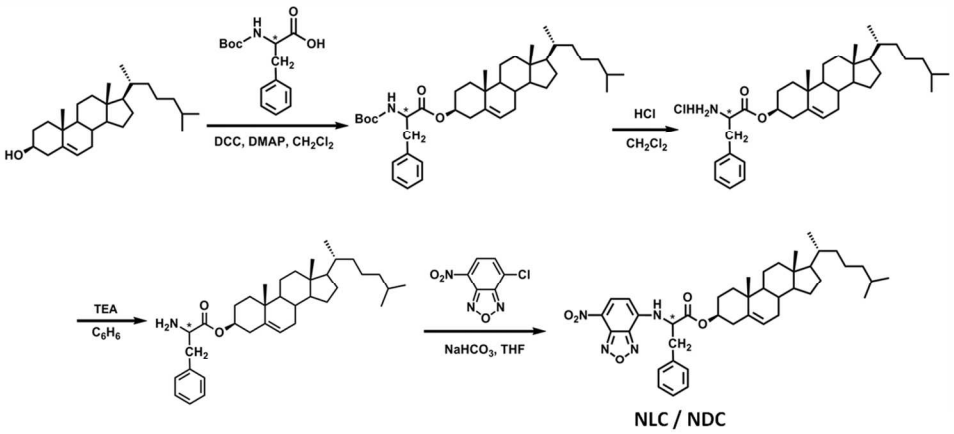

Scheme 1 Schematic representation of the synthesis of two nitrobenzoxadiazole (NBD)-containing cholesteryl (Chol) derivatives, of which L/D-phenylalanine was used as a linker **(NLC** and **NDC)**.

Unlike physical stimuli, most of the responses triggered by chemical stimuli are hard to be reversed. Furthermore, chemical stimuli may cause contamination to the gel systems under study due to residues remained after the chemical interactions. Therefore, exploring gel systems that response to chemical stimuli, and the response is reversible without extra chemical addition is a significant challenge in the area of supramolecular gel research. It is believed that this kind of gels will find important real-life applications. [25]

To create LMMGs-based molecular gels with diverse functionalities, cholesterol (Chol) and nitrobenzoxadiazole (NBD) were specially chosen as main building blocks. This is because Chol has been proven as an efficient structural unit to enhance self-assembly of its derivatives in solution state no matter the liquid is hydrophilic or hydrophobic, and NBD is a widely used fluorophore for imaging and sensing in life science due to its sensitivity to environmental changes and high fluorescence quantum yield.[26,27] Combination of the two residues has been proven to be an efficient strategy to develop new LMMGs with superior properties. [28] For example, we, for the first time, took NBD as a main building block for the creation of new LMMGs, and introduced it into some ALS type Chol derivatives. In this way, several excellent gel systems with amazing mechanical strength and self-healing properties were developed. Inspired by the discovery, two kinds of NBD appended cholesteryl derivatives with L(D)-phenylalaninate as linkers (**NLC**, **NDC**) were designed and synthesized. The gelation behaviors of them in 34 liquids were tested to explore the effect of spatial configuration on the gelation. Based upon the test, the system of **NDC**/DMSO was chosen as an example gel. The structure, the formation mechanism, the rheological property, and the fluorescence behavior of the gel system were studied systematically. It was found with surprising that the fluorescence emission of the gel is super-sensitive to the presence of ammonia, and the response is fast and fully reversible. Accordingly, an "ammonia leaking" monitor was created. This paper reports the details.

Experimental Section

1. Preparation of NLC and NDC

The methods used for the preparation of **NLC** and **NDC** are schematically shown in Scheme 1. Specifically, cholesteryl L-phenylalaninate with a primary amine group in its end was synthesized according to a previous report.[29] The compound (1.07 g, 2 mmol) was further reacted with NBD-Cl (0.40 g, 2 mmol), which had been dissolved in 20 mL of THF, under stirring in the presence of $NaHCO_3$ (0.20 g, 2.4 mmol) at room temperature. The reaction was monitored by TLC and conducted for another 24 h. After the reaction, the mixture was filtered and the filtrate was evaporated to dryness. The residue as obtained was purified by a silica gel column chromatography with THF/petroleum ether (1:6, v/v) as elute to give desired product as orange powders in 70% yield. The procedures used for the preparation of **NDC** are similar to that for **NLC**. Satisfactory results were also obtained.

For **NLC**: Yield 70%. ^{1}H NMR ($CDCl_3$/Me_4Si, 400 MHz): 8.39-8.41 (d, 1H, H-Ar), 7.29-7.31 (d, 2H, H-Ar), 7.17-7.19 (3H, d, H-Ar), 6.57-6.55 (d, H, NH), 6.04-6.02 (d, 1H, H-Ar), 5.38-5.39 (d, H, alkenyl), 4.66-4.72 (m, 2H, C-H), 3.23-3.38 (m, 2H, Ph-CH_2), 0.68-2.33 (m, 44H, cholesteryl protons). (Fig. S1). Elemental analysis, calcd. for $C_{42}H_{56}N_4O_5$: C, 72.38; H, 8.10; N, 8.04. Found: C, 72.20; H, 8.15; N, 7.98%.

For **NDC**: Yield 70%. ^{1}H NMR ($CDCl_3$/Me_4Si, 400 MHz): 8.39-8.41 (d, 1H, H-Ar), 7.29-7.30 (d, 2H, H-Ar), 7.16-7.18 (3H, d, H-Ar), 6.54-6.55 (d, H, NH), 6.04-6.02(d, 1H, H-Ar), 5.38-5.39 (d, H, alkenyl), 4.67-4.75(m, 2H, C-H), 3.22-3.38 (m, 2H, Ph-CH_2), 0.68-2.32 (m, 44H, cholesteryl protons). (Fig. S2). Elemental analysis, calcd. for $C_{42}H_{56}N_4O_5$: C, 72.38; H, 8.10; N, 8.04. Found: C, 72.44; H, 8.04; N, 7.89%.

2. Gelation test

A known weight (0.025 g) of a tested compound and a measured volume (1 mL) of selected pure liquid were placed into a sealed test tube and the system was sonicated at room temperature for 30 min, then the test tube was inversed to observe if a gel had been formed. Gels obtained after sonication at room temperature were denoted as "G*". If the result was negative, the test tube was heated until the solid was dissolved completely, and then the system was cooled to room temperature in air. Finally, the test tube was inversed to observe if the solution inside could still flow. A positive test is obtained if the flow test is negative. A gel was denoted as "G" (gel), a mixture of gel and solution was referred to as "PG" (partial gel), and a system in which only solution remained was denoted as "S" (solution). For those, of which heating results in dissolution, but cooling was accompanied by precipitation, the systems were referred to as "P" (precipitation). Systems in which the gelators could not be dissolved even at the boiling point of the liquid were defined as "I" (insoluble).

3. Gel-sol phase transition temperatures (T_{gel})

Falling drop method was employed to measure T_{gel}. The gels were placed in the inverted tubes, then they will fall under the influence of gravity when heated to a certain temperature in an oil bath.[30]

4. Scanning electron microscopy (SEM) studies

SEM images of the xerogel were taken on a TM3000 Tabletop micr-oscope (Hitachi Limited). The accelerating voltage was 15 kV and the emission current was 10.0 mA. The xerogel for the measurement was prepared by freezing the gel formed in the concerned liquid at a measured concentration in liquid nitrogen, and evaporated by a vacuum pump for 24 h. Before the examination, the sample was coated with a thin layer of gold.

5. ^{1}H NMR measurements

The sample containing a gelator under test and deuterated reagent was prepared in an NMR tube, which was detected by a Fourier Digital NMR spectrometer (AVANCE 400 MHz) at a given temper-ature between 298 K and 338 K or at a given concentration range from 0.1 to 0.25% (w/v). The temperature-/concentration- dependent ^{1}H NMR spectra were recorded in DMSO-d_6 to investigate the gelation mechanism. For characterization studies, the ^{1}H NMR spectra of the compounds were measured in $CDCl_3$.

6. FTIR measurements

All FTIR measurements were performed on a Bruker VERTEX 70 V infrared spectrometer in an attenuated total reflectance (ATR) mode. KBr pellets were obtained by mixing a small amount of the dried gel samples and anhydrous KBr powder. And the solution sample was prepared by dropping a dilute solution of the sample on a hot KBr disc, and then evaporating the solvent immediately.

7. Rheological measurements

Rheological measurements were carried out with a stress-controlled rheometer (TA instrument, AR-G2) equipped with a steel-coated parallel-plate geometry (20 mm diameter). The gap between two plates was 1 mm. A liquid trapping device was used to minimize the evaporation. The measurements were conducted after the sample was placed on the plate for 30 min at 25 ℃.

Firstly, a stress sweep measurement at fixed frequency was conducted, which provides the information about the mechanical strength of the gel sample. Secondly, the storage modulus, G', and the lose modulus, G'', were monitored as functions of frequency from 0.1 to 628.0 rad s^{-1} at a constant stress of 10 Pa well within the linear visco-elastic region.

The thixotropic study was conducted to examine the alteration in the rheological properties of the gel under the application and release of shear. This process includes two steps: (1) Deformation: a constant oscillatory shear stress (5000 Pa) that is enough to destroy the gel was applied to the gel for 2 min; (2) Modulus recovery in a time sweep: the high shear force was removed and a very small monitoring shear stress of 10 Pa was exerted on the destroyed gel for 2 min. The storage modulus G' and the loss modulus G'' of the system were monitored with the change of time.[31]

8. UV-Vis and Circular dichroism (CD) measurements

UV-Vis and CD spectra were obtained using chirascan circular dichroism spectrometer. In the measurement, the hot solution was poured into a quartz cell (0.1 mm) and cooled to room temperature to form a stable gel (1%, w/v). The temperature- dependent UV-Vis and CD spectra were recorded, and the concentration-dependent UV-Vis and CD spectra were also recorded at 25 °C.

9. Hansen solubility parameters studies

Hansen solubility parameters (HSPs) are available for each liquid and quantify liquid's interaction ability via dispersion, dipole–dipole, and hydrogen bonding. With the Nanomaterials Laboratory Hansen Solubility Parameter Data Fitting Software, 3-D plots showing regions of solubility (S), gelation (G) and insolubility (I) were constructed for the system of **NDC** in different liquids at a given temperature and concentration, which may allow us to predict if a compound gels a given liquid or not. [32, 33]

10. Fluorescence measurements

Fluorescence measurements were performed on a time-correlated single photon counting Edinburgh FLS 920 fluorescence spectrome-ter at room temperature. The film was adhered to the wall of a sealed quartz cell.

Results and discussion

1. Gelation behaviors

The gelation behaviors of **NLC** and **NDC** in 34 liquids were tested at a standard concentration of 2.5% (w/v), and the results are shown in Table S1. With reference to the table, it is seen that there is a huge difference in the gelation behavior of them. Specifically, **NDC** gels seven of the liquids tested, whereas **NLC** gels none of them, indicating that the chirality of the phenylalanine residue, which connects the chol unit and the NBD residue, shows a great effect upon the gelling performances of the compounds since the compositions and basic structures of them are the same. The data of critical gelation concentrations (CGCs) and sol-gel phase transition temperatures (T_{gel}) of the gels are also listed in the table.

With further reference to Table S1, it is found that **NDC** gels DMSO, kerosene, acetonitrile and several alcohols, but only the **NDC**/DMSO gel exhibits good stability and high mechanical strength. Furthermore, its CGC is only 0.3% (w/v), suggesting great efficiency of **NDC** in gelling of the liquid. As expected, incorporation of NBD endows the gels bright fluorescence under light irradiation, which may provide a possibility for them to find practical uses.

2. Scanning electron microscopy (SEM) studies

The micro-structures of the gel networks are important both for understanding the self-assembly processes and for finding their practical applications. Accordingly, the morphologies of the xerogels or aggregates from the **NDC**/DMSO systems with different compositions were examined by SEM. Some typical images are shown in Fig. 1. Reference to the images reveals that with increasing the concentration of **NDC**, the aggregates change from loose fibers

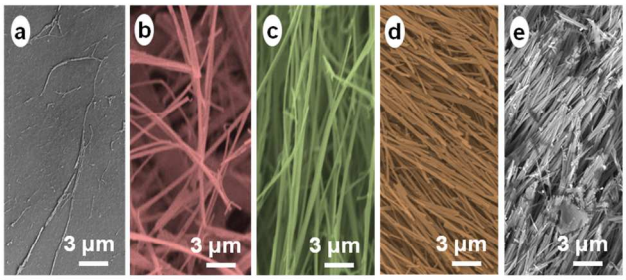

Fig. 1 SEM images of the **NDC**/DMSO gel system with different concentrations of NBD: (a) 0.05%, (b) 0.50%, (c) 1.00%, (d) 2.50% , (e) 5.00% (w/v).

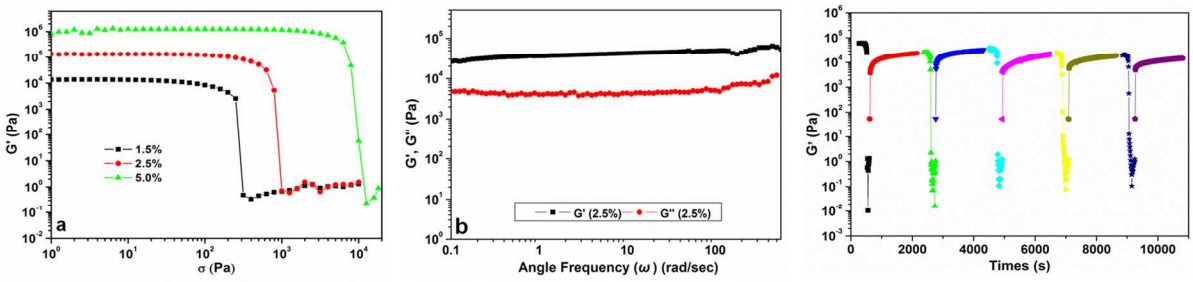

Fig. 2 (a) Evolution of G' as a function of the applied shear stress at different concentrations of **NDC** in DMSO; (b) Evolution of G' and G'' as functions of angle frequency; (c) Evolution of G' as a function of time. The sample under test is **NDC**/DMSO gel.

to highly ordered fiber arrays, suggesting that the structures of the aggregates can be modulated by simple variation of the gelator concentration, which may provide convenience for device making, a necessity for functionality studies. [34-37]

3. Rheological studies

The rheological property of a gel is extremely important for its real-life uses. [38-42] Therefore, the properties of the gels created were studied by taking **NDC**/DMSO as an example gel system. The results from stress sweep of different concentrations of the gelator are shown in Fig. 2a, of which the sweep was conducted at a constant frequency of 1.0 Hz and at 25 □. It is revealed that with increasing the gelator concentration from 1.5% to 5.0% (w/v), the value of G', associated with the energy storage, increased from 1.39×10^4 Pa to 8.26×10^5 Pa and the yield stress increased from 248.6 Pa to 8381.0 Pa, a result as expected and of value for practical uses, such as crystal growth and device fabrication.[43,44]

Frequency sweep is important for examining the ability of a material to tolerate external forces. [45] Accordingly, the gel of **NDC**/DMSO (2.5%, w/v) was employed to conduct the test at a shear stress of 10 Pa, which is well within the liner region of the gel sample, and the result is shown in Fig. 2b. Reference to the figure reveals that with the angle frequency increased from 0.1 rad s^{-1} to 555.0 rad s^{-1}, the values of the storage modulus (G') are always higher than those of the loss modulus (G''), associated with the loss of the energy. Furthermore, both G' and G'' were kept relatively stable within the whole frequency region swept, suggesting that there had been no phase transition during the sweep process and the gel possesses good tolerance to external forces.

To examine the thixotropic property of the gel, further rheological measurements were conducted alternatively under a shear stress (5000 Pa) significantly greater than the corresponding yield stress and no shear stress. The results are shown in Fig. 2c. With reference to the figure, it is seen that the gel recovers immediately after removing the shear stress. This sol–gel phase transition process can be repeated for at least five times, indicating that the gel is thixotropically reversible. This property might be valuable for some specific applications such as injection molding, drug delivery, etc.[46, 47]

4. ^{1}H NMR and FTIR spectroscopy studies

Temperature-/concentration-dependent ^{1}H NMR measurements were conducted in order to obtain further information about the formation mechanism of the gel networks due to their effectiveness in confirming hydrogen-bonding formation.[38] The results are shown in Fig. 3. With reference to Fig. 3a, it is seen that the signal of N-H proton appeared at 9.28 ppm at 328 K, but it shifted to 8.98 ppm at 368 K, an indication of existence of hydrogen bonds in the gel networks. However, it is not clear wither the hydrogen bonds formed inter-molecularly or intra-molecularly. To reveal the origin of the hydrogen bonding, concentration-dependent ^{1}H NMR spectroscopy measurements were also conducted, and the results are shown in Fig. 3b. It is seen that the signal of N-H proton is too weak to be seen when the concentration of the gelator is set at 0.1% (w/v). The signal appears at 9.06 ppm when the concentration is increased to 0.18% (w/v). The signal shifted to 9.03 ppm when its concentration is increased to 0.5% (w/v), a result in support of inter-molecular interaction. In addition, the signals of NBD protons at 8.46 ppm and 6.45 ppm slightly shifted down-field to 8.48 ppm and 6.47 ppm, respectively, with increasing the gelator concentration from 0.10% to 0.5% (w/v), a result also found in temperature-dependent ^{1}H NMR studies, indicating that in addition to the presence of inter-molecular hydrogen-bonding, π-π stacking also plays important role for the formation of the **NDC**/DMSO gel.

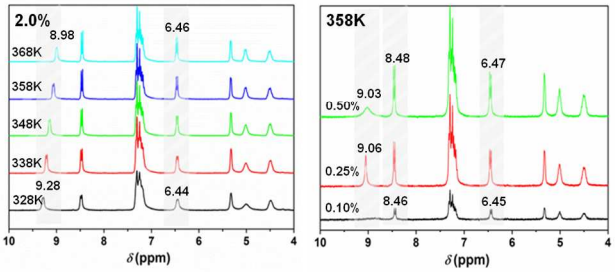

Fig. 3 (a) Temperature-dependent ^{1}H NMR spectra of **NDC** in DMSO-d_6, and (b) concentration-dependent ^{1}H NMR spectra of **NDC** in DMSO-d_6.

FTIR spectroscopy can also provide profitable information on the formation of hydrogen bonds during the gelation process. Accordin-

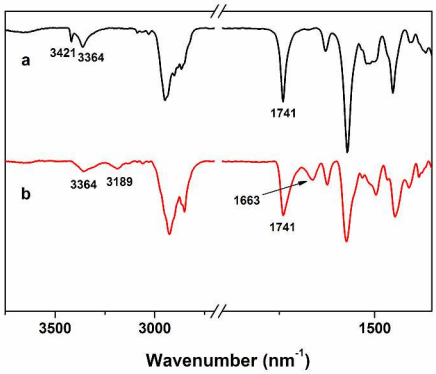

Fig. 4 FTIR spectra of **NDC** in its THF solution (a), and in its DMSO gel (1.0%, w/v) (b).

gly, the FTIR spectrum of **NDC**/DMSO in gel state and that of **NDC**/THF in solution state were recorded and the results are shown in Fig. 4. With reference to the traces shown in the figure, it is seen that the stretching vibration of the N-H bond and that of the C=O bond of **NDC** in THF appeared at 3364 cm^{-1} and 1741 cm^{-1}, respectively. Upon gelation, however, the bands shifted to 3189 and 1663 cm^{-1}, respectively, suggesting existing of hydrogen bonds within the gel, another driving force to promote the gel formation.

5. UV-Vis and CD spectroscopic studies

UV-Vis spectroscopy study is a useful technique to elucidate the interaction among gelator molecules, and even can be used to distinguish different aggregation mode such as H- or J- aggregation. Accordingly, concentration- and temperature-dependent absorption spectra of the DMSO solution or gel of **NDC** were recorded. The results are shown in Fig. S3. With reference to Fig. S3a, it is clearly seen that the position of the maximum absorption of NBD shows an obvious red-shift along with increasing the gelator concentration from 0.18% (sol state) to 0.50% (gel state), an indication of π-π stacking and J-type aggregation. To verify the tentative conclusion, temperature-dependent absorption spectroscopy studies were also conducted, and the results are shown in Fig. S3b. It is obvious that the maximum absorption of NBD exhibits significant red-shift with decreasing the temperature from 338 K (sol state) to 298 K (gel state), a result in support of the conclusion obtained from the concentration-dependent measurements, and confirms again that the structure of NBD possesses a strong tendency to form aggregates in solution.[28]

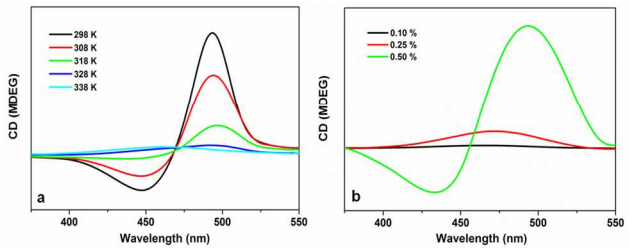

Fig. 5 Temperature-dependent CD spectra of **NDC**/DMSO system at a concentration of 1.0 % (w/v) (a), and concentration-dependent CD spectra of the system recorded at room temperature (b).

It is known that circular dichroism (CD) can be used to study not only molecular chirality but also the chirality of a superamolecular aggregate.[48] Considering the importance of chirality to the gelation behavior of **NDC** and **NLC**, temperature- and concentration-dependent CD spectroscopy studies of the gel systems were conducted. The results are shown in Fig. 5. It is obvious that the sample is CD-active in gel state at 298 K, but the CD signal decreased gradually and eventually disappeared at sol state with increasing the temperature from 298 K to 338 K, indicating that the CD signal observed originated from the chirality of the gel networks, the aggregates of the gelator, rather than from the inherent chirality of the molecules of the gelator (*cf.* Fig. 5a).[49] This result is further supported by the results from concentration-dependent CD spectroscopy studies because the sample is only CD-active at concentrations greater than its CGC, a minimum requirement for gelation (*cf.* Fig. 5b).

6. Hansen solubility parameters studies

Hansen solubility parameters (HSPs) studies can help us to understand the reasons why a gel forms and predict whether the gelator under study gels a given liquid or not. For this reason, the Hansen space of the systems under study was constructed by using the Hansen Solubility Data Fitting Software, the so called "concentric sphere shell fit method".[32] The results are shown in Fig. 6.

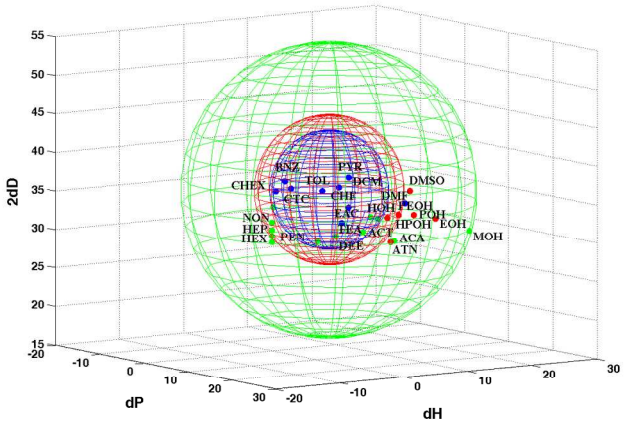

Fig. 6 Solubility data for **NDC** in the liquids represented in Hansen space with spheres/shells, where blue stands for the soluble space, red the gel space, and green the insoluble one. The dots marked in different colors are from the results shown in Table 1. Again, the colors have same meaning with those described for the space or spheres.

According to the definition of solubility parameter by Hildebrand, the overall energy density (δ) can be separated into three components, which are dispersive (δ_d), polar (δ_p) and hydrogen-bonding (δ_h), respectively (eq. 1):

$$\delta = \sqrt{\delta_d^{\,2} + \delta_p^{\,2} + \delta_h^{\,2}} \qquad (1)$$

The HSPs parameters for the liquids shown in Table S1 were obtained from literatures.[31] To be simple, the systems of the liquids with 2.5% (w/v) of **NDC** were classified into three categories, which are soluble (S), gel (G) and insoluble (I), respectively. Partial gels, precipitates, and suspensions were treated as "insoluble". The distances (R) between the gelator (δ_p, δ_h and δ_d) and those of a liquid (δ_p^l, δ_h^l and δ_d^l) in Hansen space were calculated using eq. 2.

$$R = \sqrt{4(\delta_d - \delta_d^l)^2 + (\delta_p - \delta_p^l)^2 + (\delta_h - \delta_h^l)^2} \qquad (2)$$

In the Hansen spaces, the solution sphere (blue) are nearest to the center, the gel shells (red) are next, and the insoluble shells (green) are outmost. Generally speaking, the liquids fit within the proper sphere/shells (as an aside, viewing the 3-D plots in 2-D is sometimes misleading that is points that appear to be inside a given sphere may actually be outside it). However, some of the liquids points locating within the sphere/shells do not agree with the experimental results, which are believed to be an indication of difficulty of using group contribution methods in the calculation of the HSPs of a complex molecule. Moreover, the parameters as discussed do not cover all interactions between the components within a gel system. In other

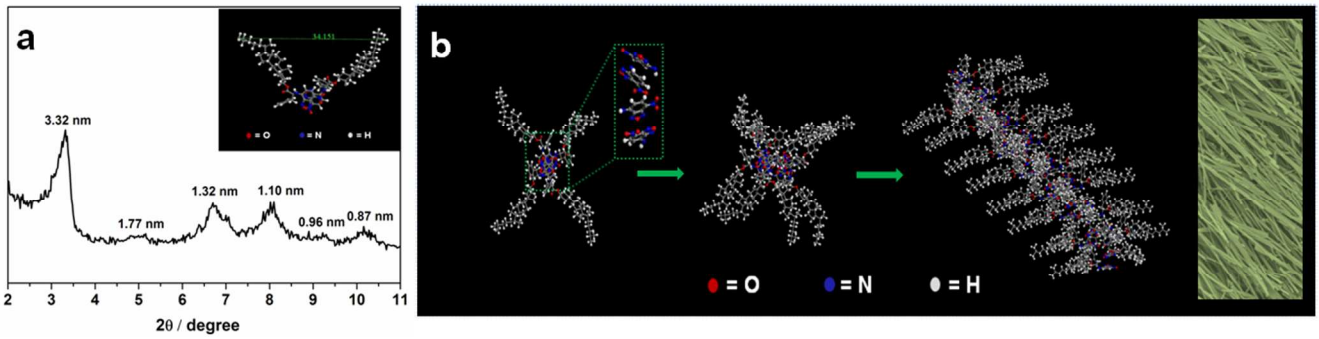

Fig. 7 (a) XRD profile of **NDC**/DMSO (1.0%, w/v) and the primary assembly structure of a packing unit (inset). (b) Possible packing mode of the fibrous aggregates of **NDC**/DMSO gel.

words, there are some other factors which also affect gelation, for example, π-π stacking. However, valuable information can be still acquired from the analysis. For the systems under study, it is found that among the three parameters only δ_H exhibits a good linear relationship with the T_{gel} of **NDC** in the liquids under study (*cf*. Fig. S4), indicating the importance of hydrogen-bonding formation for the gelation of the systems.

7. XRD studies

In order to elucidate the detailed packing mode of the gelator in the gel networks at a molecular level, XRD measurement of the xerogel of **NDC**/DMSO was performed. The result is shown in Fig. 7. Reference to the trace shown in the figure reveals that it is characterized by six reflection peaks, corresponding spacings (*d*) of 3.32, 4.99, 6.71, 8.02, 9.21 and 10.16 nm, respectively, which follow the ratio of 1: (1/ √ 2) : (1/2) : (1/ √ 5) : (1/3) : (1/ √ 8), suggesting that **NDC** aggregated in a tetragonal way [50] and the length of a basic structural unit is 3.32 nm, which approximately equals to the length of a dimer of **NDC** (*cf*. Fig. 7a). Considering the interactions between the gelator molecules revealed by FTIR, ^{1}H NMR and XRD studies, a model representing the assembly of **NDC** in DMSO was proposed (*cf*. Fig. 7b).

8. Sol-gel phase transition

One of the most promising properties that molecular gels can offer is a stimulated response leading to reversible sol–gel phase transition.[20] During the primary test of the fluorescence behavior of **NDC** gels, it was found by chance that the phase transition of the **NDC**/DMSO gel to sol can be simply induced by bubbling ammonia. Interestingly, the reversed process is realized after evaporation of the gas (*cf*. Fig. 8). The process can be repeated for many times. Interestingly, the reversed process is realized after evaporation of the gas (*cf*. Fig. 8). The process can be repeated for many times.

Further reference to the figure reveals that the ammonia-triggered sol–gel phase transition was accompanied with fluorescence quenching, and the quenching was reversed upon evaporation of the ammonia introduced. It is to be noted that the fluorescence quenching was not found in temperature-induced phase transition.

To explore the mechanism of the fluorescence quenching induced by ammonia vapor, ^{1}H NMR measurement was conducted. Firstly, the DMSO-d_6 solution of **NDC** at a concentration of 1.0% (w/v) was prepared in a NMR tube. Secondly, ammonia vapor was injected into the tube, which was accompanied by gel-sol phase transition and fluorescence quenching. The ^{1}H NMR spectra recorded before and after ammonia gas injection are shown in Fig. 9. Compared with the results from the temperature- and concentration-dependent ^{1}H NMR measurements (*cf*. Fig. 3), of which the changes of the signals triggered by the phase transition is slight, the changes of the proton signals of NBD unit in this case are obvious, shifted from 8.50 and 6.39 ppm to 7.69 ppm and 5.88 ppm, respectively. At the same time, some other changes were also observed. For example, the signal of N-H disappears. Considering the results revealed, it is reasonable to believe that it is the interaction of ammonia and the nitro group of NBD that causes the fluorescence quenching and the gel-sol phase

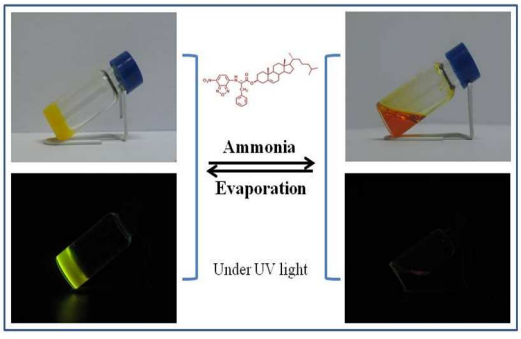

Fig. 8 Reversible gel-sol phase transition of the **NDC**/DMSO gel via injection of ammonia and evaporation of the gas (a), and the accompanied fluorescence quenching and fluorescence recovery (b).

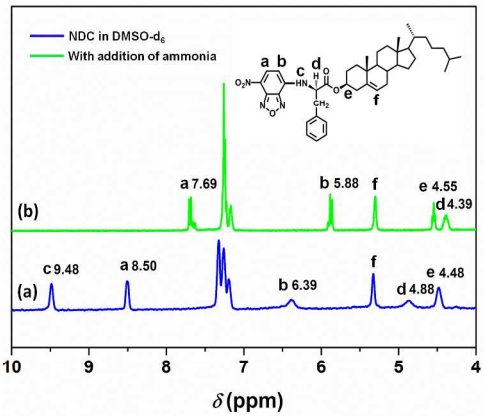

Fig. 9 (a) ^{1}H NMR spectrum of **NDC** in DMSO-d_6, (b) ^{1}H NMR spectrum of **NDC** in DMSO-d_6 with addition of ammonia.

transition.

The discovery is of great importance for conducting functionality-oriented supra-molecular gel research. For example, an ammonia sensing film had been fabricated by in-situ growth of the **NDC** nanostructures via coating the **NDC**/DMSO gel on a glass plate surface. To examine the sensing performance of the film, a conceptual device for monitoring "ammonia leaking" had been developed (*cf*. Fig. S5). As shown in a short video (*cf*. Video S1), the system works very well, and what is even happier, the sensing can be repeated for many times. A detailed study is under progress.

Conclusion

Two NBD-containing Chol derivatives with L-/D-phenyl alanine in the linkers were designed and synthesized. Gelation tests demonstrated that the L-phenyl alanine containing compound, **NLC**, does not gel any of the liquids tested, but the one with D-phenyl alanine in the linker, **NDC**, gels 7 of the 34 liquids tested. Interestingly, the gel networks of **NDC**/DMSO gel are characterized by highly ordered fiberous array structures, and show remarkable thixotropic properties. More interestingly, it was found that introduction of ammonia gas could result in gel-sol phase transition and fluorescence quenching of the gel system. The non-fluorescent solution as resulted, however, could be reverted immediately to fluorescent gel upon evaporation of the ammonia gas. On the basis of the discovery, an ammonia sensing film had been fabricated, and the film-based "ammonia leaking" monitoring device was developed. Preliminary test demonstrated that performance of the system is exceptional good, a typical and persuasive example to show the important real-life applications of molecular gels.

Acknowledgements

We thank the Natural Science Foundation of China (91027017, 21273141, and 21206089) and the Program for Changjiang Scholars and Innovative Research Team in University (IRT1070).

Notes and references

† Key Laboratory of Applied Surface and Colloid Chemistry (Ministry of Education), School of Chemistry and Chemical Engineering, Shaanxi Normal University, Xi'an, 710062, P. R. China

DOI: 10.1039/b000000x/

1 A. Wynne, M. Whitefield, A. J. Dixon and S. Anderson, *J. Dermatol Treat.*, 2002, **13**, 61-66.
2 I. Tokarev and S. Minko, *Soft Matter*, 2009, **5**, 511-524.
3 P. Baglioni, L. G. Dei, E. Carretti and R. Giorgi, *Langmuir*, 2009, **25**, 8373-8374.
4 L. kumar, R. P. Singh, S.G. Singh and D. kumar, *Int. J. Pharm. Sci. Rev. Res.*, 2011, **9**, 83-91.
5 M. Jaiswal, S. Lale, N. G. Ramesh and V. Koul, *React. Funct. Polym.*, 2013, **73**, 1493-1499.
6 N. Yan, G. He, H. L. Zhang, L. P. Ding and Y. Fang, *Langmuir*, 2010, **26**, 5909-5917.
7 K. Q. Liu and J. W. Steed, *Soft Matter*, 2013, **9**, 11699-11705.
8 M. Xue, D. Gao, K. Q. Liu, J. X. Peng and Y. Fang, *Tetrahedron*, 2009, **65**, 3369-3377.
9 B. K. An, D. S. Lee, J. S. Lee, Y. S. Park, H. S. Song and S. Y. Park, *J. Am. Chem. Soc.*, 2004, **126**, 10232-10233.
10 K. K. Kartha, S. S. Babu, S. Srinivasan and A. Ajayaghosh, *J. Am. Chem. Soc.*, 2012, **134**, 4834-4841.
11 C. M. Yu, M. Xue, K. Q. Liu, G. Wang and Y. Fang, *Langmuir*, 2014, **30**, 1257-1265.
12 V. Bhalla, A. Gupta, M. Kumar, D. S. S. Rao and S. K. Prasad, *Appl. Mater. Interfaces*, 2013, **5**, 672-679.
13 J. W. Chung, B. K. An and S. Y. Park, *Chem. Mater.*, 2008, **20**, 6750-6755.
14 X. Z. Yan, F. Wang, B. Zheng and F. H. Huang, *Chem. Soc. Rev.*, 2012, **41**, 6042.
15 L. X. Jiang, Y. Yan and J. B. Huang, *Soft Matter*, 2011, **7**, 10417-10423.
16 M. Piepenbrock, G. O. Lloyd, N. Clarke and J. W. Steed, *Chem. Rev.*, 2010, **110**, 1960.
17 Y. Hisamatsu, S. Banerjee, M. B. Avinash, T. Govindaraju and C. Schmuck, *Angew. Chem. Int. Ed.*, 2013, **52**, 12550-12554.
18 X. D. Yu, L. M. Chen, M. M. Zhang and T. Yi, *Chem. Soc. Rev.*, 2014, **43**, 5346-5371.
19 C. Wang, Q. Chen, F. Sun, D. Q. Zhang, G. X. Zhang, Y. Y. Huang, R. Zhao and D. B. Zhu, *J. Am. Chem. Soc.*, 2010, **132**, 3092-3096.
20 Y. Hisamatsu, S. Banerjee, M. B. Avinash, T. Govindaraju and C. Schmuck, *Angew. Chem. Int. Ed.*, 2013, **52**, 12550-12554.
21 S. Samai and K. Biradha, *Chem. Mater.*, 2012, **24**, 1165-1173.
22 M. M. Zhang, D. H. Xu, X. Z. Yan, J. Z. Chen, S. Y. Dong, B. Zheng and F. H. Huang, *Angew. Chem. Int. Ed.*, 2012, **51**, 7011-7015.
23 H. Shao, C. F. Wang, J. Zhang and S. Chen, *Macromolecules*, 2014, **47**, 1875-1881.
24 M. George and R. G. Weiss, *J. Am. Chem. Soc.*, 2001, **123**, 10393-10394.
25 R. G. Weiss, *J. Am. Chem. Soc.*, 2014, **136**, 7519-7530.
26 S. R. Liu and S. P. Wu, *J. Fluoresc.*, 2011, **21**, 1599-1605.
27 G. D. Zhou, H. L. Wang, Y. Ma and X. Q. Chen, *Tetrahedron*, 2013, **69**, 867-870.
28 Z. Y. Xu, J. X. Peng, N. Yan, H. Yu, S. S. Zhang, K. Q. Liu and Y. Fang, *Soft Matter*, 2013, **9**, 1091-1099.
29 Y. G. Li, K. Q. Liu, J. Liu, J. X. Peng, X. L. Feng and Y. Fang, *Langmuir*, 2006, **22**, 7016-7020.
30 A. Takahashi, M. Sakai and T. Kato, *Polym. J.*, 1980, **12**, 335-341.
31 X. Y. Hou, D. Gao, J. L. Yan, Y. Ma, K. Q. Liu and Y. Fang, *Langmuir*, 2011, **27**, 12156.
32 K. K. Diehn, H. Oh, R. Hashemipour, R. G. Weiss and S. R. Raghavan, *Soft Matter*, 2014, **10**, 2632-2640.
33 N. Yan, Z. Y. Xu, K. K. Diehn, S. R. Raghavan, Y. Fang and R. G. Weiss, *J. Am. Chem. Soc.*, 2013, **135**, 8989-8999.
34 G. Bao and S. Suresh, *Nat. Mater.*, 2003, **2**, 715-725.
35 M. M. Stevens and J. H. George, *Science*, 2005, **310**, 1135-1138.
36 J. C. Tiller, *Angew. Chem. Int. Ed.*, 2003, **42**, 3072-3075.
37 S. Mizrahi, J. Gun, Z. G. Kipervaser and O. Lev, *Anal. Chem.*, 2004, **76**, 5399-5404.
38 J. Brinksma, B. L. Feringa, R. M. Kellogg, R. Vreeker and J. v. Esch, *Langmuir*, 2000, **16**, 9249-9255.
39 P. Kirilov, F. Gauffre, S. F. Messant, E. Perez, I. R. Lattes, *J. Phys. Chem. B*, 2009, **113**, 11101-11108.
40 M. Lescanne, P. Grondin, A. d'Aléo, F. Fages, J. L. Pozzo, O. M. Monval, P. Reinheimer and A. Colin, *Langmuir*, 2004, **20**, 3032-3041.

41 P. D. Sawant and X. Y. Liu, *Chem. Mater.*, 2002, **14**, 3793-3798.
42 A. Dawn, T. Shiraki, H. Ichikawa, A. Takada, Y. Takahashi, Y. Tsuchiya, L. T. N. Lien and S. Shinkai, *J. Am. Chem. Soc.*, 2012, **134**, 2161-2171.
43 K. C. Mevada, V. D. Patel and K. R. Patel, *Arch. Phys. Res.*, 2012, **3**, 258-263.
44 S. Diring, F. Camerel, B. Donnio, T. Dintzer, S. Toffanin, R. Capelli, M. Muccini and R. Ziessel, *J. Am. Chem. Soc.*, 2009, **131**, 18177-18185.
45 X. Q. Cai, K. Q. Liu, J. L. Yan, H. L. Zhang, X. Y. Hou, Z. Liu, Y. Fang, *Soft Matter*, 2012, **8**, 3756-3761.
46 A. Rudert and R. Schwarze, *J. Non-Newtonian Fluid Mech.*, 2009, **161**, 60-68.
47 P. K. Vemula, J. Li and G. John, *J. Am. Chem. Soc.*, 2006, **128**, 8932-8938.
48 N. Harada, S. L. Chen and K. Nakanishi, *J. Am. Chem. Soc.*, 1975, **17**, 5343-5352.
49 P. F. Duan, H. Cao, L. Zhang and M. H. Liu, *Soft Matter*, 2014, **10**, 5428-5448.
50 J. J. van Gorp, *Helices by hydrogen bonding: folding and stacking of chiral supramolecular scaffolds*, Technische Universiteit Eindhoven, 2004.

TOC of the manuscript

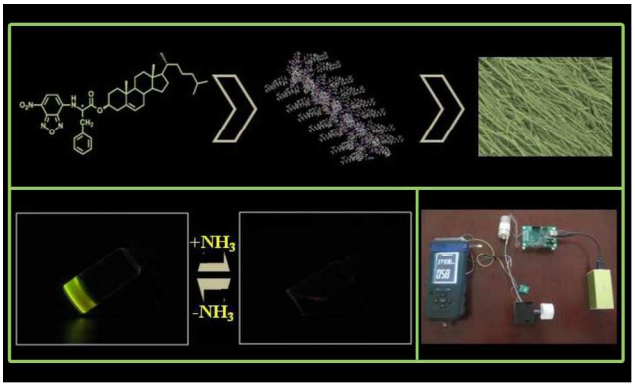

A fluorescent gel with ultra-fast and fully reversible response to the presence of ammonia gas is presented, and based upon the gel a conceptual "ammonia leaking" monitor was developed.